Journal of Hazardous Materials 132 (2006) 26–38

Journal of Hazardous Materials

www.elsevier.com/locate/jhazmat

Wind-induced dust generation and transport mechanics on a bare agricultural field☆

Ted M. Zobeck [a,*], R. Scott Van Pelt [b]

[a] *Wind Erosion and Water Conservation Research Unit, USDA, Agricultural Research Service, 3810 4th Street Lubbock, TX 79415, USA*

[b] *Wind Erosion and Water Conservation Research Unit, USDA, Agricultural Research Service, 302 W I-20, Big Spring, TX 79720, USA*

Available online 19 January 2006

Abstract

Strong atmospheric winds may cause wind erosion and dust emissions on bare, dry, erodible fields. Since these dust emissions may exceed particulate matter limits established by the United States Environmental Protection Agency, information on dust generation and transport mechanics is needed to determine the particulate hazard of dust sources. Measurements of climatic variables and airborne sediment mass and concentration were made during three strong wind events on a bare, fine sandy loam field in west Texas. This study clearly shows that dust flux estimates were very sensitive to dust concentration measurement height. PM_{10} flux values estimated between heights of 2 and 5 m were 2–5 times those estimated between heights of 5 and 10 m. Tower placement in relation to the upwind unerodible boundary produced significant differences in dust flux that varied with storm intensity. During the most intense storm event, the PM_{10} flux between heights of 2 and 5 m measured at the tower 200 m from the unerodible boundary was almost 2.5 times as that measured at the tower 100 m from the unerodible boundary. Vertical PM_{10} dust flux was closely related with horizontal sediment flux only when the winds came from the same direction during the entire duration of horizontal sediment flux measurements.

Keywords: PM_{10}; Fugitive dust; Dust flux; Wind erosion; Air quality

1. Introduction

The Clean Air Act, amended in 1990, required the US Environmental Protection Agency (USEPA) to establish National Ambient Air Quality Standards (NAAQS). These standards set limits on airborne pollutants, including particulate matter, considered harmful to the public and the environment. The standards were designed to protect public health and welfare, including protection against decreased visibility, damage to animals, crops, vegetation, and buildings [1]. Particulate matter is subdivided by size. Particles with a mass median aerodynamic diameter of less than 10 μm are called PM_{10} and particles with a mass median aerodynamic diameter of less than 2.5 μm are called $PM_{2.5}$. PM_{10} particles pose health risks because they can be inhaled into the respiratory system and the $PM_{2.5}$ pose a greater risk because they can be inhaled deeply into the lungs. Although many pollutants originate from industrial and other anthropogenic sources, geologic materials may contribute significant airborne particulate matter.

Much is known and has been written about wind as a geological process causing aeolian sediment transport and deposition of particulate matter [2–6]. Interest continues in this topic as shown by recent conferences in Africa and West Asia [7], Europe [8] and the United States [9]. Airborne particles originating from geologic materials can have many sources and may pose threats to humans and animals, depending upon the size and geochemistry of the particles and any materials adsorbed onto the particles. In this paper, we limit our discussion to the emission and transport of suspended particles (or fugitive dust) from earth surfaces due to the force of the wind, a process often called wind erosion. Although sources of suspended dust are numerous and varied, similar processes occur when

☆ Mention of trade names or commercial products in this article is solely for the purpose of providing specific information and does not imply recommendation or endorsement by the US Department of Agriculture.

* Corresponding author. Tel.: +1 806 723 5240; fax: +1 806 723 5272.
E-mail address: tzobeck@Lbk.ars.usda.gov (T.M. Zobeck).

0304-3894/$ – see front matter © 2005 Elsevier B.V. All rights reserved.
doi:10.1016/j.jhazmat.2005.11.090

dust is emitted from deserts, dry lake beds, agricultural fields, dirt roads, construction sites, and other areas where the surface is bare and erodible particles are exposed to the force of winds.

Particles moved by the wind can range up to about 1 mm in diameter, but particles travelling great distances are usually much smaller (<100 μm). Particles of fine dust (<20 μm) have a low settling velocity, even under low wind speeds, and may be transported great distances and kept suspended in the atmosphere for a very long time [10]. Wind erosion is a significant source of fine dust and PM_{10}, particularly in regions of highly erodible soils [11–13].

Field studies of airborne dust produced at or near the origin of intense dust sources are difficult to conduct yet numerous studies have been reported [14–22]. Most studies have focused on total suspended dust <20 μm. However, due to the interest in PM_{10} in the NAAQS, recent studies in the US have focused on PM_{10} emissions [20–24].

Fine dust is generally emitted due to the force of saltating particles impacting the soil surface [6,14,25]. Recent work in silty loessial soils of the US Pacific Northwest suggests that fine dust may also be entrained into the atmosphere due to the direct force of the wind, without saltation bombardment [24]. Work by Gillette et al. [20] has related horizontal mass flux of sediment to the vertical flux of PM_{10} particles for a large sandy playa lake in California. The lake represents an unusual large eroding surface. Information on the vertical flux of PM_{10} particles is needed to determine the potential particulate hazard of eroding surfaces. Since the USEPA designated the southern half of the Owens Valley as a 'Serious' PM_{10} non-attainment area, a State Implementation Plan was developed that calls for the control of dust on 43 km^2 of the lake bed [23].

However, most eroding surfaces are often much smaller than the Owens Lake bed and the study of suspended dust poses significant challenges. If the field is very small, the total amount of emitted dust may be determined by simply measuring the vertical profile of dust concentrations of the plume and multiplying by the wind speed to obtain a horizontal flux. However, this may not be practical if the field is so large that the entire plume cannot be sampled or estimated or if there are many heterogeneous source areas in large fields.

Many studies use the gradient method, described by Gillette [26], to estimate vertical flux of suspended dust. The application of the gradient method in agricultural fields is not clear. The method requires measurement of dust at two heights and seems to assume a fully developed dust plume, yet no studies have described the effect of dust sensors height or placement in relation to a developing dust plume close to the dust source on vertical dust flux measurements. In addition, agricultural fields are often so variable or small that horizontal emissions are not uniform. In this paper, we test the hypothesis that large variations in vertical dust flux may arise depending upon sensor and tower placement in a small agricultural field. In addition, we describe the effect of horizontal mass flux on vertical dust flux in small fields and demonstrate the importance of wind direction and sampler placement.

2. Materials and methods

2.1. Experimental site

The study site was located in the southern Great Plains of west Texas at the United States Department of Agriculture, Agricultural Research Service (USDA-ARS), Wind Erosion and Water Conservation Research Unit field station in Big Spring, Texas (32.2702N, 101.4865W). The climate is semiarid with a mean annual temperature of 17.1 °C, mean annual precipitation of 470 mm and mean annual wind speed of 8 m s^{-1}. The study was conducted on an Amarillo fine sandy loam (13% clay, 78% sand and 0.3% organic carbon) classified as a fine-loamy, mixed, thermic, superactive Aridic Paleustalf [27]. These Late Quaternary surface sediments have been significantly modified by aeolian processes [28].

The 3-ha (100 m radius) round study field was chiseled, planed and maintained in a bare, flat condition for the duration of the study (Fig. 1). The field was surrounded by 10 ridges approximately 0.3 m high and 1 m apart. The ridges were established to stop saltating particles from entering or leaving the field. Previous research demonstrated that soil loss on a sandy soil in west Texas was reduced 90% with ridges up to 2.5 m high [29]. In addition, fields upwind and down wind of the study field were maintained in an unerodible condition during the study period.

2.2. Instrumentation

The study was conducted in March 2003. Three dust storm dates (March 4, 18 and 27) were selected for detailed analysis. On these dates, wind erosion was measured using a combination of saltation/creep and Big Spring Number Eight (BSNE) samplers (Fig. 2). On March 4, BSNE saltation sampler clusters [30] were used at the center and east locations (Fig. 1). BSNE saltation sampler clusters consist of a series of BSNE passive saltation samplers located at heights of 0.05, 0.10, 0.20, 0.5, and 1.0 m above the soil surface (Fig. 2).

Combination saltation/creep samplers were also located at the center and east positions. The saltation/creep samplers [31] are passive samplers with 0.005 m wide openings at heights of

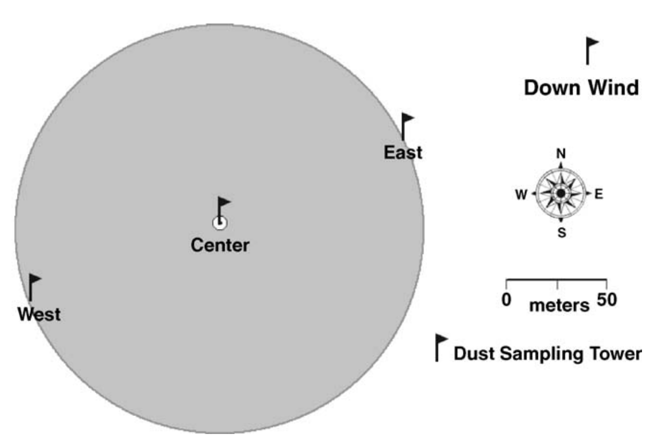

Fig. 1. Location of dust sampling towers in relation to eroding field (shaded).

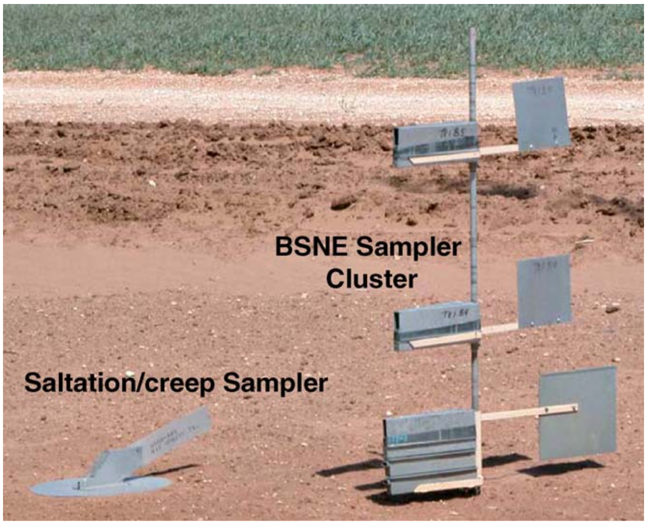

Fig. 2. Saltation/creep and BSNE samplers used to collect horizontal mass flux.

0–0.003, 0.003–0.009, and 0.009–0.02 m (Fig. 2). Data from the lowest opening were not complete so only the two higher sampling heights were used for this sampler. The mean sampling heights of the openings were 0.006 and 0.015 m. These samplers orient into the wind and particles are blown horizontally into the sampler. The mass of sediment collected in each sampler was measured after each day with a dust storm. Saltating particles were also detected with a SENSIT® particle impact detector [32] located in the center of the field. The SENSIT uses a piezoelectric crystal to detect saltating sand grains at a frequency of 1 Hz. In this study, the piezoelectric crystal was positioned at the soil surface.

Suspended dust was measured using DustTrak® (TSI, Inc.) aerosol monitors mounted on towers at 2, 5, and 10 m heights. Three towers were available for use in this study. Towers were located at the west, center and east positions, respectively, on March 4 (Fig. 1). Since this first observation date showed incoming dust level to be quite low and relatively uniformly vertically distributed, the west tower was moved to a down wind location 100 m east of the east tower for the March 18 and 27 observation dates. Although useful information was gained by the west tower, we felt more information would be gained by using this tower in a down wind position. The towers were located along a line running from 240° to 60° magnetic north. DustTrak monitors measure the concentration of PM_{10} using laser light scattering. The DustTraks were modified by adding a 1.9 mm diameter orifice that oriented into the wind. The orifice was sized to provide isokinetic sampling for ambient wind speeds of 10 m s^{-1} (Fig. 3). Some reduction in sampling efficiency may have occurred for winds substantially above or below this level. The DustTraks were activated during specific daylight hours during dust storm dates and sampled at 1 Hz frequency (Table 1). Sufficient memory capacity was not available to run the DustTraks continuously for more than 6 h. To evaluate the effect of saltation on dust emissions, SENSITS and DustTraks clocks were synchronized.

Fig. 3. DustTrak sampling head and instrument enclosure (top) and close-up of sampling head orifice.

Table 1
Observation summary data during 2003 dust flux measurements

Date	Time of observation (hh:mm)	Total minutes (min)	Mean 2 m wind speed (m s^{-1})	Mean maximum wind gust[a] (m s^{-1})	Mean wind direction (°)	Mean threshold wind speed (m s^{-1})	Mean z_0[b] (m)	Standard error z_0 (m)	Mean u^*[b] (m s^{-1})	Standard error u^* (m s^{-1})
March 4	11:55–18:30	395	8.0	11.5	256	10.0	0.0006	0.0001	0.44	0.013
March 18	10:23–14:23	240	8.5	10.9	258	9.7	0.0003	0.0000	0.36	0.0097
March 27	10:10–14.45	275	7.0	8.9	252	8.8	0.0004	0.0001	0.4	0.019

[a] Wind gust expressed as mean 2 m wind velocity plus 2× standard deviation.
[b] z_0, aerodynamic roughness; u^*, friction wind speed.

Wind direction was measured at the center of the field with a wind vane at 2 m height and wind speed was measured at heights of 0.5 and 2.0 m with cup anemometers. A standard US National Weather Service meteorological station was located in an adjacent field approximately 100 m south of the study field.

2.3. Parameter calculation

One minute wind velocity observations averaged over 20-min periods were used to estimate friction velocity, u^* ($\mathrm{m\,s^{-1}}$), and aerodynamic roughness, z_0 (m), using the equation:

$$U(z) = \frac{u^*}{k} \ln\left(\frac{z}{z_0}\right) \tag{1}$$

where $U(z)$ is wind speed ($\mathrm{m\,s^{-1}}$) at height z (m) and k is von Karman's dimensionless constant (0.4) [33]. The mean values of wind speed at 2 m height, friction velocity and aerodynamic roughness over the entire sampling period for each date are shown in Table 1. These values do not exactly fit Eq. (1) because they are the average values of many 20-min sampling periods, over which time the values in Eq. (1) may vary due to slight differences in wind direction, wind speed, and other factors.

Threshold wind velocity for each 1-min period was calculated using the equation proposed by Stout [34]:

$$u_\mathrm{t} = u_\mathrm{mean} - \sigma N^{-1}(\gamma) \tag{2}$$

where u_t is threshold wind speed ($\mathrm{m\,s^{-1}}$), u_mean the mean wind speed, σ the standard deviation of the wind speed, and $N^{-1}(\gamma)$ is the inverse of the normal distribution function of the saltation activity, γ. The saltation activity was calculated as the fraction of time in which saltation activity was detected with the SENSIT. For example, if saltation was detected for 30 s during the 60 s over which wind speed was measured, the saltation activity was calculated as 0.5.

The vertical flux (F_v, $\mathrm{mg\,m^{-2}\,min^{-1}}$) of PM_{10} suspended dust was calculated according to the gradient method of Gillette [14] as described by Rajot et al. [35] using the equation:

$$F_\mathrm{v} = \frac{u^* k (C_\mathrm{b} - C_\mathrm{t})}{\ln\left(\frac{z_\mathrm{t}}{z_\mathrm{b}}\right)} \tag{3}$$

where C_b and C_t are the concentrations ($\mathrm{mg\,m^{-3}}$) of PM_{10} at the bottom and top DustTraks, respectively, and z_b and z_t are the heights of the bottom and top DustTraks, respectively.

The horizontal flux of saltation material was calculated using the method of Stout and Zobeck [19]. Eroding material collected by the saltation/creep and BSNE samplers was used to determine the horizontal flux ($\mathrm{kg\,m^{-1}\,event^{-1}}$) applying:

$$F_\mathrm{h}(z) = F_{z=0}\left(1 + \frac{z}{\beta}\right)^{-2} \tag{4}$$

where $F_\mathrm{h}(z)$ is the horizontal mass flux at height z, $F_{z=0}$ is horizontal mass flux at the soil surface, and β is a scale height parameter. The $F_{z=0}$ and β parameters were determined by taking the square root of both sides of Eq. (4) to yield:

$$F_\mathrm{h}(z)^{-0.5} = F_{z=0}^{-0.5}\left(1 + \frac{z}{\beta}\right) \tag{5}$$

Plotting the inverse of the square root of the mass of sediment caught in the saltation samplers ($F_\mathrm{h}(z)^{-0.5}$) as a function of sampler height will yield a straight line within the fully developed portion of the mass saltation flux profile [19]. In this study, BSNE samplers at heights of 0.0065, 0.015, 0.05, 0.10, and 0.20 m were used to determine horizontal mass flux. The slope and intercept of this line was used to determine the $F_{z=0}$ and β parameters. Flux at the surface ($F_{z=0}$) was equal to the intercept^{-2} and β was equal to intercept/slope.

Pearson correlations were performed using the analysis feature of Microsoft Excel 2002®.

Tests for normality of data were performed using the Proc Univariate procedure in the SAS statistical analysis system, version 8 [36].

3. Results and discussion

A summary of the wind profile characteristics determined for periods when saltation was active and dust concentration measurements were collected is listed in Table 1. Dust concentration measurements were collected in the late morning and early afternoon on each day.

The observation periods ranged from 240 to 395 min long. The wind originated from the west–southwest (252–258° mean wind direction) on all days. The mean 2 m wind speeds were lower than the mean threshold wind speeds during the same period of saltation and dust measurement (Table 1), demonstrating the importance of wind gusts. Since we did not measure maximum wind speeds during 1-min observations, we attempted to estimate the maximum wind gust using the mean and the standard deviation of the wind speed. The mean maximum wind gust in Table 1 represents the wind speed calculated as the mean wind speed plus two times the standard deviation of the mean. Since analyses indicated that the wind speed data were normally distributed, only about 2.5% of wind speed values exceeded the estimated maximum wind gust as calculated above.

3.1. Relation of dust concentration, flux and saltation

3.1.1. March 4 observations

The relation of vertical PM_{10} dust flux and saltation can be observed by comparing SENSIT counts (SC) with observed dust concentration or dust flux (Table 2). Correlations of SENSIT counts with Table 2 parameters were made only during times when SENSIT and dust concentration data were both available as shown in Table 1. As described above, the memory resources did not allow us to continuously collect PM_{10} concentration data for more than 6 h so the DustTraks were manually started during each storm. Differences in time of observation were caused by differences in natural storm characteristics. Although the mean wind speed and observation durations varied among storm dates, the wind directions were about the same (Table 1).

Table 2
Pearson correlation coefficients of SENSIT counts with PM_{10} by date and tower location

Tower location	Source	2 m PM_{10} concentration	5 m PM_{10} concentration	10 m PM_{10} concentration	$PM_{10}flux_{2-5}$ [a]	$PM_{10}flux_{5-10}$
March 4, 2003						
West	SENSIT counts	0.11	−0.06	0.01	0.31	−0.14
Center (modified)[b]	SENSIT counts	0.67	0.37	−0.31	0.72	0.62
Center (unmodified)[b]	SENSIT counts	0.66	0.13	−0.12	0.65	–[c]
East (modified)	SENSIT counts	0.69	0.66	0.26	0.77	0.68
March 18, 2003						
Center[d]	SENSIT counts	0.42	0.33	0.26	0.40	0.32
East[d]	SENSIT counts	0.47	0.42	0.33	0.48	0.44
Down wind[d]	SENSIT counts	0.47	0.47	0.39	0.47	0.43
March 27, 2003						
Center	SENSIT counts	0.56	0.33	0.41	0.63	0.24
East	SENSIT counts	0.76	0.31	0.35	0.63	0.7
Down wind	SENSIT counts	0.53	0.73	0.59	0.30	0.59

[a] $Flux_{2-5}$ is flux calculated using Eq. (3) and heights 2 and 5 m; $flux_{5-10}$ is flux calculated using Eq. (3) and heights 5 and 10 m.
[b] Modified data were modified by subtracting west tower PM_{10} value at corresponding time and height.
[c] Indicates data not available.
[d] SENSIT counts correlated after subtracting 2 min from recorded time.

The March 4 west tower dust concentration by height, SC, vertical PM_{10} flux calculated using Eq. (3) comparing different concentration heights, and average 2 m wind speed are shown in Fig. 4. The data shown in Figs. 4–7 represent 1-min average values. Higher frequency comparisons were beyond the scope of this study. Since the west tower was on the upwind side of the field (Fig. 1), we assume mainly PM_{10} originating off the study field was observed. The PM_{10} concentrations at all heights appear similar and have no apparent relation with SC (Fig. 4).

SENSIT counts were much better correlated with wind and PM_{10} variables at the center tower on March 4 (Fig. 5 and Table 2). Increases in PM_{10} concentration at the 2 and 5 m heights closely followed increases in SC (Fig. 5). The correlation of SC with PM_{10} concentration at 2 m height was 0.67. The correlation of SC with PM_{10} concentration measured at a heights of 5 m ($R = 0.37$) and 10 m ($R = -0.31$) were lower. The $PM_{10}flux_{2-5}$ was well-correlated ($R = 0.72$) with SC. The correlation of $PM_{10}flux_{5-10}$ was not as well but still correlated ($R = 0.62$).

Observed values of $PM_{10}flux_{2-5}$ and $PM_{10}flux_{5-10}$ were quite different at the center tower on March 4. The $PM_{10}flux_{2-5}$ was about 3.6 times that of the $PM_{10}flux_{5-10}$ value (Table 3). The reason for this result is clarified by examination of Fig. 5. The PM_{10} concentration at 2 m height was about an order of magnitude higher than the concentrations at the 5 or 10 m heights. Clear differences in dust concentration distribution with height produced the differences in PM_{10} flux values.

SENSIT counts were somewhat better correlated with wind and PM_{10} variables at the east tower than the center tower on March 4 (Table 2). The east tower was located 100 m east of the SENSIT location. The PM_{10} concentration of the east tower at the 10 m height (not shown) showed a small but visible response to the SC not observed in the PM_{10} concentration of the10 m height of the center tower (Fig. 5). Apparently, the PM_{10} plume had not yet reached the 10 m height near the SENSIT located at the center of the field but did rise to 10 m at the east end of the field. The development of this plume is shown by the greater PM_{10} flux values at the east tower, which were about 2.5–3 times the values observed at the center tower (Table 3). As with the center tower, the $PM_{10}flux_{2-5}$ of the east tower was greater (about 2.7 times) than the $PM_{10}flux_{5-10}$ values. Visual observations on this date indicated that dust plumes reached the 10 m height of the east tower infrequently. The dust plume did reach the 5 m height frequently at the east tower.

The March 4 PM_{10} concentration values shown in Fig. 5 were modified by subtracting the PM_{10} concentration observed at the same height at the west tower from corresponding heights at the center and east towers. This modification generally improved the correlation of SC with PM_{10} concentration and flux values. For example, before modification, the correlation of SC with 2 m PM_{10} concentration was 0.66, correlation of SC with 5 m PM_{10} concentration was 0.13, and correlation of SC with PM_{10} flux measured at 2–5 m heights was 0.65. After subtracting the west tower PM_{10} values at corresponding heights, correlations of dust concentration at 5 m and the $flux_{2-5}$ values are improved. Unfortunately, only one test date was available to make this correction and subsequent test dates do not apply the modification. Additional testing the usefulness of this modification is needed.

SENSIT counts were correlated with the March 4 1-min average 2 m wind velocity with a correlation of 0.58. We surmised that the average 1-min 2 m wind velocity tended to reduce the variation in wind velocity by masking higher frequency gustiness. We attempted to introduce this variation with the estimated maximum wind gust in this paper. However, the correlation of wind speed with saltation was only slightly improved ($R = 0.61$) when the estimated maximum wind gust was used in the correlation. Correlation of SC with higher frequency wind velocity measurements are needed to improve this relation and are in progress.

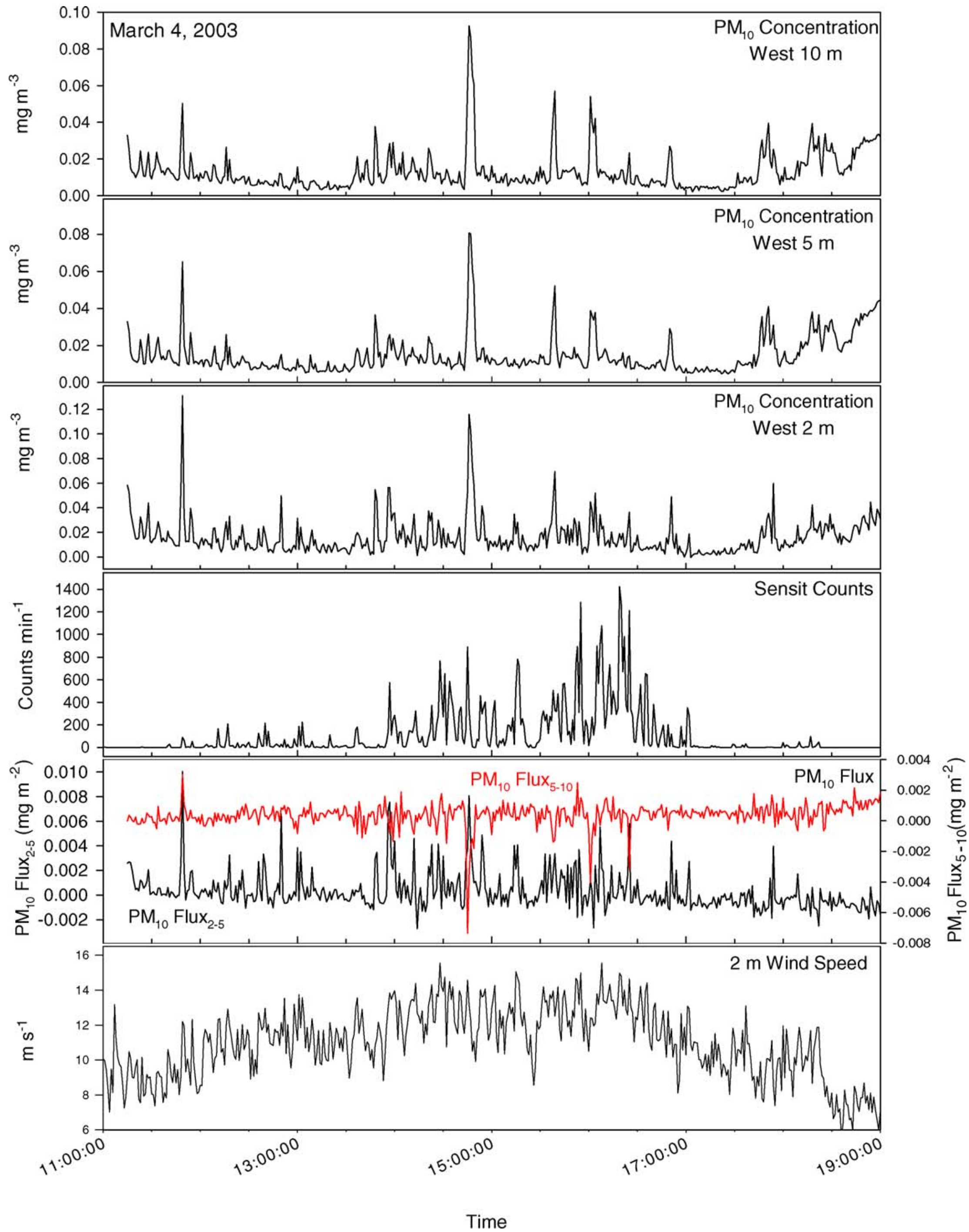

Fig. 4. PM_{10} concentration by sampler height, SENSIT counts, estimated PM_{10} flux for two height intervals, and 2 m wind speed for the west tower on March 4, 2003. All values are 1-min means of data collected every second.

3.1.2. March 18 observations

After the March 4 test date, the west tower was moved 100 m down wind of the east tower location (Fig. 1). PM_{10} dust concentration values were collected at the center, east and down wind towers on March 18 and 27. As discussed above, since the west tower was not available to provide background data after the March 4 test, March 18 and 27 data were not modified to remove incoming suspended dust.

Pearson correlation coefficients for most of the March 18 PM_{10} data were not as high as those found for the March 4 data (Table 2). Part of the difference is attributed to the background level of PM_{10} included in the March 18 observations. Some of the differences may also be related to an apparent lack of precise synchronization of clock times for the SENSIT and the PM_{10} sensors on March 18. Comparisons of the SENSIT counts and PM_{10} at 2 m concentrations on March 18 suggest an apparent lag in the SENSIT counts. Direct correlations of

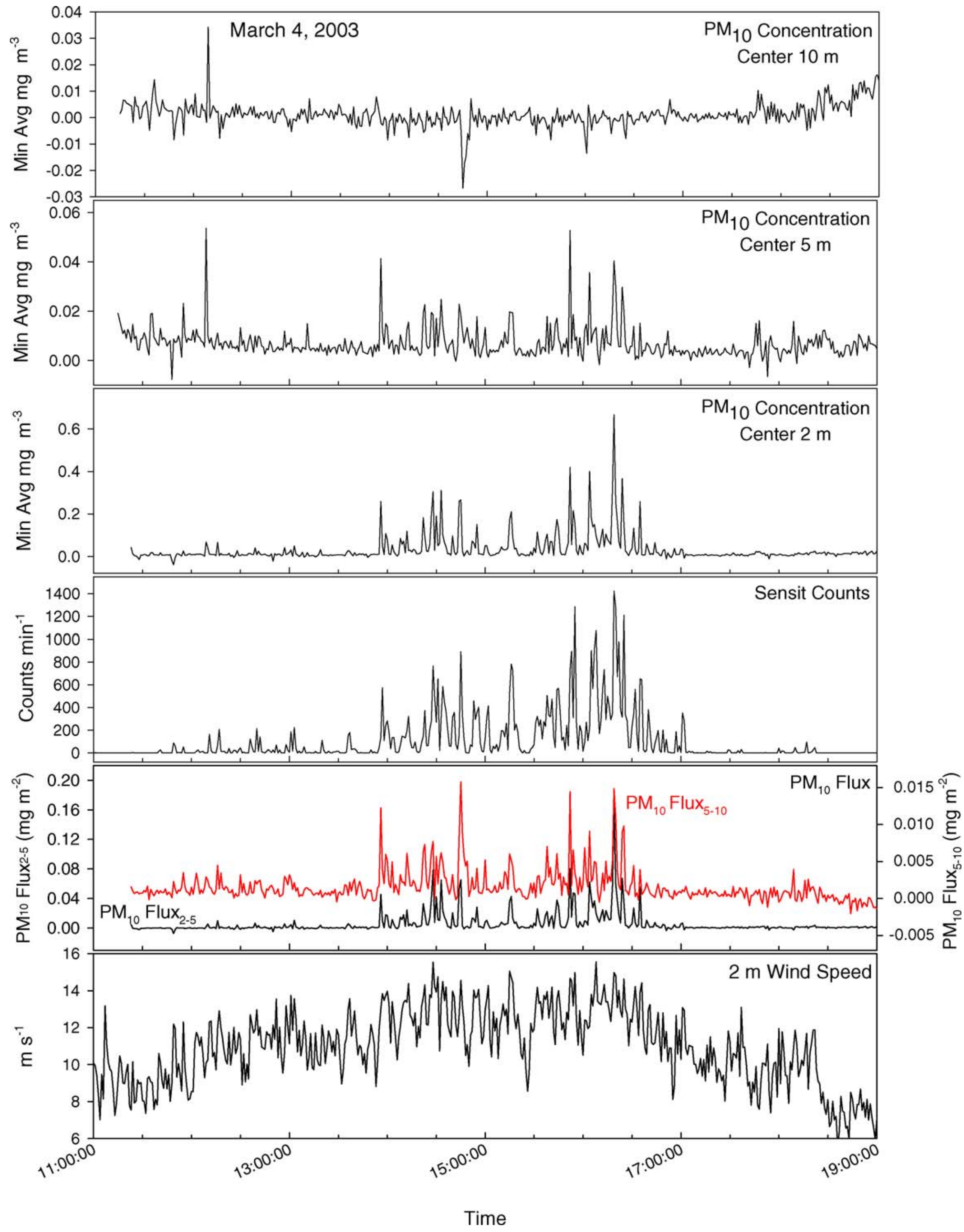

Fig. 5. PM_{10} concentration by sampler height, SENSIT counts, estimated PM_{10} flux for two height intervals, and 2 m wind speed for the center tower on March 4, 2003. All values are 1-min means of data collected every second.

SENSIT counts with PM_{10} variables were about half the values of correlations when 2 min were subtracted from each SENSIT count times (Table 1). The origin of this time lag in not known. This possible experimental error may have been caused by differences in setting of the internal clocks of the SENSIT and DustTraks. In this experiment, the clocks of both devices were set separately. In future studies, we will set all clocks using the same timing device to avoid this possible error.

Regardless of this possible error, examination of the SENSIT and PM_{10} concentration data collected at the down wind tower on March 18 shows interesting trends. As with the March 4 data, Pearson correlation coefficients of SC with dust concentration and flux values for the east tower were slightly better than correlations for the center tower on March 18 (Table 2). In addition, the PM_{10} flux values for the east tower were about 2.2–3.3 times the values measured at the same heights at the cen-

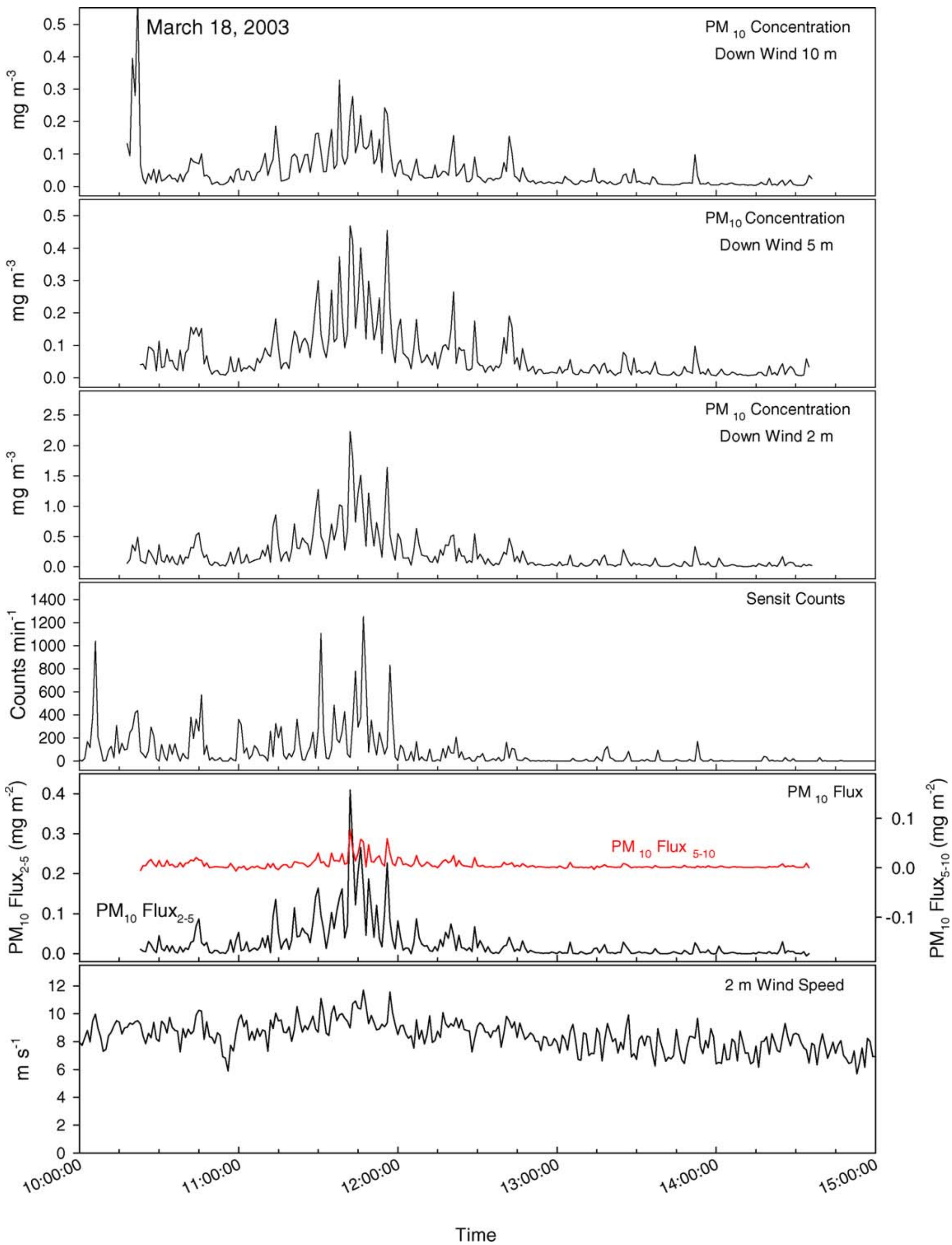

Fig. 6. PM_{10} concentration by sampler height, SENSIT counts, estimated PM_{10} flux for two height intervals, and 2 m wind speed for the down wind tower on March 18, 2003. All values are 1-min means of data collected every second.

ter tower (Table 3), again consistent with the values observed on March 4.

A down wind tower was also observed on March 18. Although the down wind tower was located in an unerodible (vegetated) area, which was 100 m down wind of the erodible field, the PM_{10} concentration data rather closely parallels the SENSIT count data (Fig. 6). The SENSIT was located about 200 m west of the down wind tower position. In addition, $PM_{10}flux_{2–5}$ at the down wind tower was 7.7 times the $PM_{10}flux_{2–5}$ recorded at the center tower and 4.6 times the $PM_{10}flux_{5–10}$ observed at the same location (Table 3).

3.1.3. March 27 observations

Pearson correlation coefficients comparing SC with PM_{10} data were higher for most of the March 27 data than those found for the March 18 data but were about the same or higher than

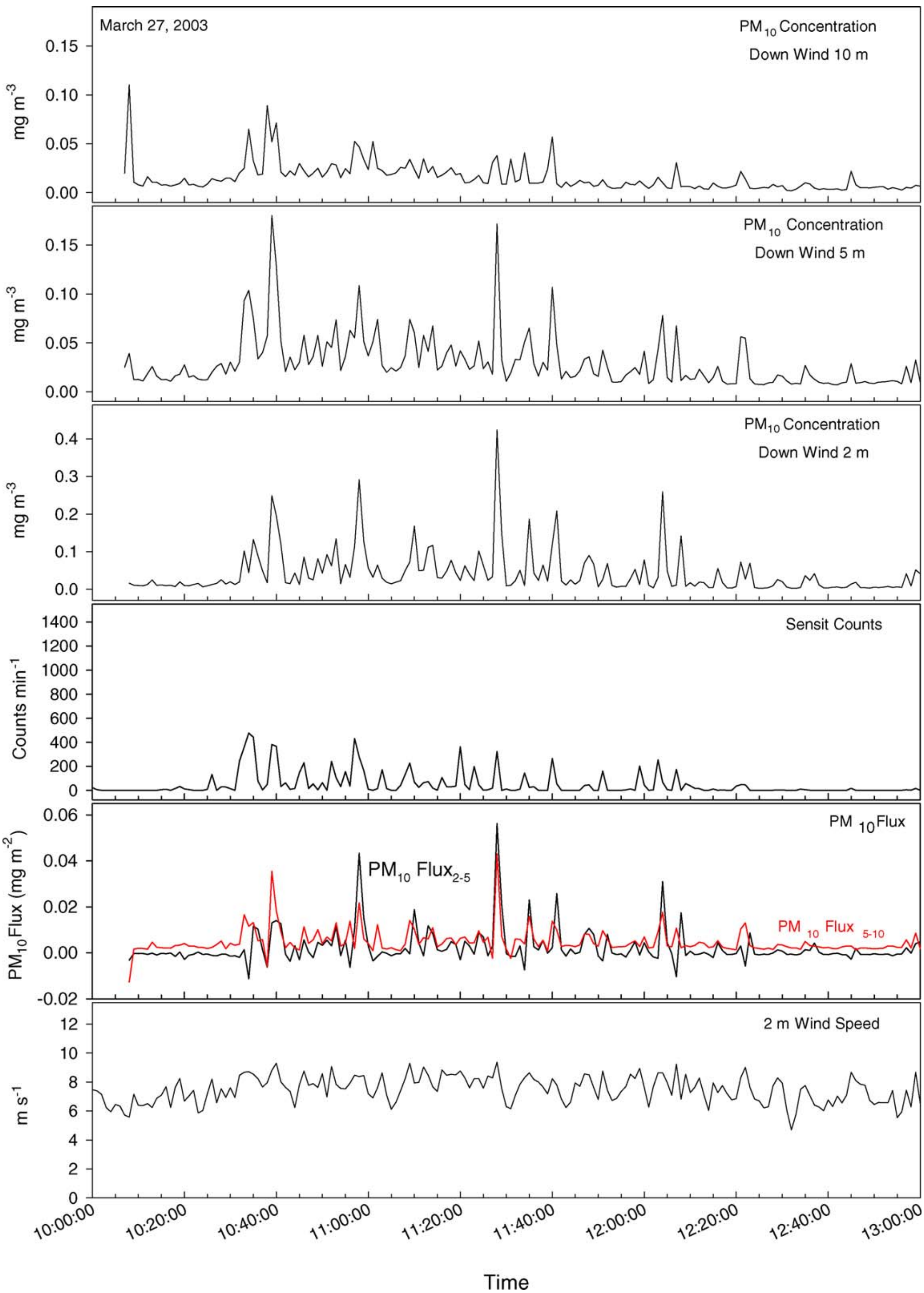

Fig. 7. PM_{10} concentration by sampler height, SENSIT counts, estimated PM_{10} flux for two height intervals, and 2 m wind speed for the down wind tower on March 18, 2003. All values are 1-min means of data collected every second.

the values for the March 4 data (Table 1). The data collected during the March 27 storm was somewhat different from that collected during the previous two storms. The time of day was approximately the same and the amount of time dust concentration data was collected during saltation activity on March 27 was greater than the March 18 storm but less than the March 4 storm (Table 1). However, the pattern of saltation during the March 27 storm was somewhat different than the other storms. The March 4 and 18 had many more SENSIT counts that were concentrated in a shorter time interval than on March 27.

Table 3
Flux observation 2003 summary data

Date	Tower location	$PM_{10}flux_{2–5}$ [a] ($mg\,m^{-2}$)	$PM_{10}flux_{5–10}$ [a] ($mg\,m^{-2}$)	$PM_{10}flux_{2–5}$ per minute ($\mu g\,m^{-2}\,s^{-1}$)	$PM_{10}flux_{5–10}$ per minute ($\mu g\,m^{-2}\,s^{-1}$)	$Flux_{2–5}/flux_{5–10}$ ratio
March 4	West	0.1216	0.1326	0.005	0.006	0.9
March 4	Center	2.5773	0.7066	0.109	0.030	3.6
March 4	East	6.3895	2.3377	0.270	0.099	2.7
March 18	Center	0.8993	0.3851	0.062	0.027	2.3
March 18	East	1.9997	1.2466	0.139	0.087	1.6
March 18	Down wind	6.9881	1.5059	0.485	0.105	4.6
March 27	Center	0.4976	0.3593	0.030	0.022	1.4
March 27	East	0.4632	0.7808	0.028	0.047	0.6
March 27	Down wind	0.3999	0.7221	0.024	0.044	0.6

[a] Total $PM_{10}flux_{2–5}$ and $PM_{10}flux_{5–10}$ were calculated by summing fluxes over the observation periods.

As a result, the PM_{10} concentrations on March 27 at the east tower were much lower than those found for the east tower on March 4 and the PM_{10} concentrations for the down wind tower were much lower on March 27 than on March 18 (compare Figs. 5–7).

Differences in dust flux estimates for different heights of dust concentration measurement were not as great March 27 as in the other observation dates. With the exception of the west tower data on March 4, the $PM_{10}flux_{2–5}$ values were from two to almost five times the values of the $PM_{10}flux_{5–10}$ values. In contract, the March 27 $PM_{10}flux_{2–5}$ values were only 40% greater than the $PM_{10}flux_{5–10}$ values at the center tower and the $PM_{10}flux_{2–5}$ values were 60% of the $PM_{10}flux_{5–10}$ values at the east and down wind towers (Table 3). In general, the PM_{10} flux values estimated for March 27 were much lower than the PM_{10} flux values on the other dates. For example, the $PM_{10}flux_{2–5}$ for the down wind tower on March 18 was 20 times that recorded for the same location on March 27.

3.2. Relation of wind speed and threshold wind speed

Wind velocity, wind direction and SENSIT counts were collected for the entire day (Fig. 8) at 1-min intervals on each observation date. Particulate matter concentration measurements were collected for much shorter periods of time due to limitations in data storage memory (Table 1). Although the wind direction was reasonably constant during dust concentration observations, it did vary substantially on each day. Threshold wind velocity measurements shown in Fig. 8 represent only time periods when it was possible to correctly calculate threshold using SENSIT and wind data. If SENSIT counts were observed for less than 2% (<2 s) or greater than 98% (>58 s) of the 1-min observation period, threshold was not determined [34].

In general, the estimated maximum wind gust and threshold wind speed decreased during the month of March (Table 1). The reason for the decrease in threshold wind speed with observation date is not clear. Wind profile calculations do not indicate significant differences in aerodynamic roughness among sampling dates. It is possible that differences due to weathering of the surface produced changes in the soil erodibility. Although very little rainfall (1.2 mm) occurred during March, resorting of loose material on the surface due to winds was significant during the month. Unfortunately, no measurements of the amount of loose erodible material were collected during this study. Cahill et al. [37] found a similar increase in dust production during an erosive period in March at Owens Lake, California. They attributed the increase to weathering and breakdown of the efflorescent (salty) crust and steady destruction of an underlying salt-silt clay crust.

Threshold values also varied within as well as among days. Although the threshold values were fairly constant on March 18, considerable variation in threshold occurred during the erosion events occurring on March 4 and 27. The difference in threshold on March 4 may be attributed to diurnal differences in relative humidity. Relative humidity approached or exceeded 90% before 9:00 and was less than 50% after 11:00. The few threshold values observed prior to 11:00 were much lower than those observed after 11:00 (Fig. 8), seeming to support the recent finding of decreased threshold velocity with increasing air humidity under some circumstances [38]. However, the effect of relative humidity is not certain since the humidity experienced in this study exceeded those observed by Ravi et al. [38].

Differences in threshold wind velocity observed on March 27 seem to be related with changes in wind direction. For most of the day, the wind was out of the southwest but changed to the north after about 19:30. When the wind changed to the north, the wind speed and threshold wind speed increased. When the wind direction changed, the area upwind of the sensors also changed. Since there was no observable difference in surface roughness in the area upwind in the north direction, the differences in threshold wind speed for erosion were likely related to spatial differences in surface soil erodibility.

3.3. Horizontal mass saltation flux

Horizontal mass flux has been associated with vertical suspended dust flux [20,25]. Horizontal mass saltation flux was measured at the center and east tower locations (Fig. 1). Total horizontal mass saltation flux was determined using Eq. (5) for saltation samplers at heights 0.006, 0.015, 0.05, 0.10, and 0.20 m. Statistics for linear regressions of height (x) and flux$^{-0.5}$, parameters in Eq. (5), and total mass flux are presented in Table 4. The center BSNE sampler was 100 m and the east sampler was

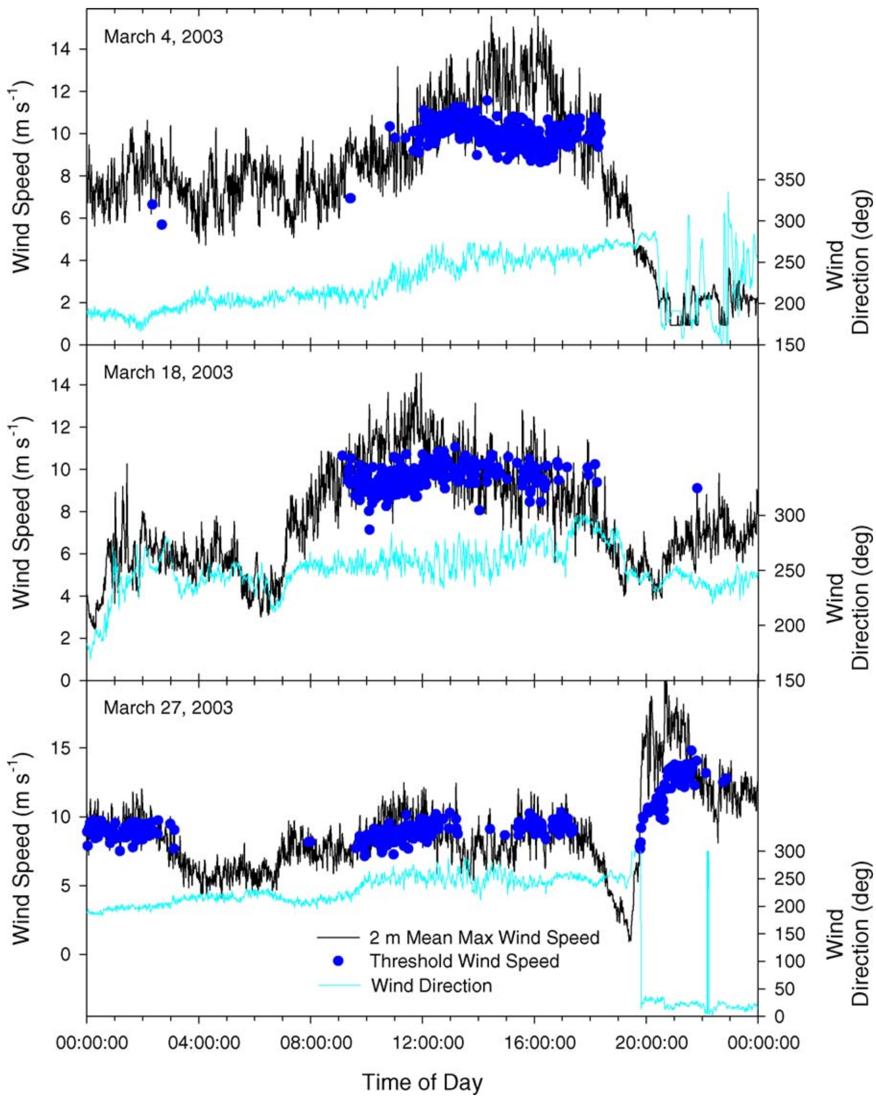

Fig. 8. Estimated maximum wind gust, threshold wind speed and wind direction on March 4, March 18 and March 27, 2003. All values are 1-min means of data collected every second.

about 190 m from the western edge of the study field. Suspended material less than 100 μm in diameter was not removed from the sample, causing some variability in correlating horizontal mass flux with suspended dust concentration. However, we assume the effect of the suspended material will be minimal because work on a similar soil in west Texas indicated that saltation size material dominates during wind erosion events at heights less than about 0.20 m [19].

Although horizontal mass flux varied by location and date, vertical $PM_{10}flux_{2–5}$ was closely related to horizontal mass flux on March 4 and 18, but not on March 27. The horizontal mass flux at the center position on March 4 was about twice that of the same location on March 18. Approximately the same variation occurred in vertical $PM_{10}flux_{2–5}$ (Tables 3 and 4). The vertical $PM_{10}flux_{2–5}$ at the center position on March 4 was 1.7 times that of the same location on March 18. The horizontal mass flux at

Table 4
Parameters used to determine 2003 total saltation flux

Date	Saltation cluster	Intercept[a]	Slope	R^2	F_0 (kg m^{-1})	Sigma (m)	Total flux (kg m^{-1})
March 4	Center	0.0296	0.3559	0.98	1141.34	0.0832	94.9
March 4	East	0.0068	0.3138	0.99	21626.30	0.0217	468.6
March 18	Center	0.0384	0.5706	0.97	678.17	0.0673	45.6
March 18	East	0.0128	0.4964	0.98	6103.52	0.0258	157.4
March 27	Center	0.0169	0.2331	0.98	3501.28	0.0725	253.8
March 27	East	0.0184	0.3869	0.98	2953.69	0.0476	140.5

[a] Equation used to calculate flux using Eq. (5) from the text. Saltation flux determined for heights 0.006–0.2 m above the soil surface.

the east position on March 4 was about three times that of same location on March 18 while the vertical $PM_{10}flux_{2–5}$ at the east position on March 4 was 1.9 times that of same location on March 18. In contrast, the vertical $PM_{10}flux_{2–5}$ was not closely related to horizontal mass flux on March 27. The horizontal mass flux at the center position on March 18 was 18% (about 1/6) that of the same location on March 27, while the $PM_{10}flux_{2–5}$ at the center position on March 18 was twice that of the same location on March 27.

In addition, the horizontal mass flux at the center position on March 27 was much greater than that observed on March 4 or 18 even though the mean wind speed and mean threshold wind speed was greater on the latter 2 days (Figs. 2 and 3). The east BSNE cluster had about half the horizontal mass flux as the center cluster on March 27. In contrast, on March 4 and 18 the east BSNE clusters collected from three to five times the sediment collected from the center BSNE cluster (Table 3).

The reason for these apparently anomalous results may be explained by knowledge of the saltation periods and wind speed in relation to the horizontal mass flux observations. Since BSNE clusters were only serviced the day following wind erosion events, the samples included sediment produced by any saltation occurring during this time period. On March 4 and 18, the wind direction was about the same during periods of saltation. On March 27 the wind direction changed dramatically at about 20:00 (Fig. 8). At this time, the wind direction changed from the southwest to north. From this direction, the fetch of the center BSNE was still about 100 m while the fetch of the east BSNE cluster changed from about 190 to 20 m. Suspension of fine dust is usually associated with saltation flux [25,26,39] and increasing fetch distance [40–43]. When the wind was coming out of the north, the center BSNE cluster was probably collecting much more sediment than the east BSNE cluster due to the much greater fetch distance. A similar increase in horizontal mass flux in the center of a field was observed when wind direction changed during an erosion study on a sandy soil in Argentina [44]. In addition, the total time of saltation flux when the BSNE clusters were collecting sediment was much greater for the center BSNE cluster on March 27 than either center BSNE clusters on March 4 or 18 (Fig. 8). A clear understanding the relation of horizontal mass flux with wind direction is necessary to unambiguously relate horizontal mass flux with other parameters such as vertical PM_{10} flux.

4. Conclusions

Estimates of vertical dust flux are often obtained by measuring dust concentrations at two heights and then applying a diffusion equation similar to Eq. (3). No standard heights at which to make dust concentration measurements are often specified. In cases where the suspended dust is thoroughly mixed with a uniform concentration near the surface in the atmospheric boundary layer, specification of measurement heights may not be needed. This was the case for the west tower on March 4. Eroding fields were not nearby and the $PM_{10}flux_{2–5}$ was about the same as the $PM_{10}flux_{5–10}$. However, this assumption is not adequate in areas with actively eroding source regions such as eroding agricultural fields or where large eroding fields contain heterogeneous areas with varying erodibility.

The results of this study clearly show that dust concentration measurements and estimates of vertical dust flux are very sensitive to measurement height in some situations. On March 4 and 18 the maximum wind gusts were greater than the threshold wind speed and there was considerably more dust near the surface than at 10 m and the $PM_{10}flux_{2–5}$ was from two to almost five times that of $PM_{10}flux_{5–10}$. However, this result was not found on March 27. On March 27, the maximum wind gust was 8.9 m s^{-1}, almost the same as the threshold wind speed of 8.8 m s^{-1}. As a result, the $PM_{10}flux_{5–10}$ was greater than $PM_{10}flux_{2–5}$ for the east and down wind towers. We believe this may be due to the greater percentage of time when no saltation was present allowing more thorough mixing of the less dense dust plume. This study suggests that the heights employed to estimate dust flux by the profile gradient method (Eq. (3)) need to be specified and/or standardized to allow better comparisons among different studies. More study is needed to determine standard measurement heights.

Vertical dust flux sampling tower location in relation to the unerodible field boundary also plays an important role in vertical dust flux estimates. A relatively small 3 ha field was used in this study.

Tower placement in relation to the upwind unerodible boundary produced significant differences in dust flux that varied with storm intensity. During the most intense storm event on March 4, the $PM_{10}flux_{2–5}$ at the east tower was almost 2.5 times as that measured at the center tower. But during the least intense storm event on March 27, the $PM_{10}flux_{2–5}$ at the east tower was a bit less than that measured at the center tower (Table 3).

This study also showed that caution should be exercised when using measurements of horizontal sediment flux to estimate vertical dust flux. Vertical dust flux was closely related with horizontal sediment flux on March 4 and 18, when the winds came from the same direction for the entire duration of horizontal sediment flux measurements. However, on March 27 the wind direction changed after vertical dust flux measurements had ceased but while the horizontal sediment flux samplers were still in the field. As a result, the vertical dust flux was not related to the horizontal sediment flux. The change in wind direction changed the fetch distance of all but the center horizontal sediment flux sampler. Since the amount of horizontal sediment flux is related to fetch distance, horizontal sediment flux samples collected from the new wind direction were no longer related to the vertical dust flux, which was all collected when the wind was blowing from a different direction.

Acknowledgements

The authors are grateful for the diligent efforts provided by Ace Berry, Charles Yates and James Davis for site installation, data collection and processing assistance. The authors also thank the anonymous reviewers for their valuable assistance in improving this manuscript.

References

[1] USEPA, United States Environmental Protection Agency, National Ambient Air Quality Standards web page, http://www.epa.gov/ttn/naaqs/, 2004 (visited June 25, 2004).

[2] R. Greeley, J.D. Iversen, Wind as a Geological Process on Earth, Mars, Venus and Titan, Cambridge University Press, Cambridge, 1985, p. 333.

[3] K. Pye, Aeolian Dusts and Deposits, Academic Press, London, 1987, p. 334.

[4] R. Cooke, A. Warren, A. Goudie, Desert Geomorphology, University College Press Ltd., London, 1993, p. 526.

[5] K. Pye (Ed.), Sediment Transport and Depositional Processes, Blackwell Scientific Publications, Oxford, 1994, p. 397.

[6] Y. Shao, Physics and Modelling of Wind Erosion, Kluwer Academic Press, Boston, 2000, p. 393.

[7] M.V.K. Sivakumar, M.A. Zobiseh, S. Koala, T. Maukonen (Eds.), Wind Erosion in Africa and West Asia: Problems and Control Strategies, Proceedings of the ICARDA/ICRISAT/UNEP/WMO Expert Group Meeting, 22–25 April 1997, Cairo, Egypt, International Center for Agricultural Research in the Dry Areas (ICARDA), Aleppo, Syria, 1998, p. 397.

[8] G. Sterk, A. Warren, Wind erosion in Europe, Catena Spec. Issue 52 (2003) 171–326.

[9] J.A. Lee, T.M. S Zobeck, Proceedings of the ICARS/GCTE-SEN Joint Meeting, Pub No. 02-2, International Center for Arid and Semiarid Lands Studies, Texas Tech University, Lubbock, TX, 2002, p. 462.

[10] D.A. Gillette, Production of dust that may be carried great distances, in: T.L. Pewe (Ed.), Desert Dust: Origin, Characteristics, and Effect on Man, The Geological Society of America, Special Paper 186, 1981, pp. 11–26.

[11] A.W. Gertler, D.A. Lowenthal, W.G. Coulombe, PM_{10} source apportionment study in Bullhead City, Arizona, J. Air Waste Manage. Assoc. 45 (1995) 75–82.

[12] D.A. Gillette, R.N. Clayton, T.K. Mayeda, M.L. Jackson, K. Sridhar, Tropospheric aerosols form major dust storms of the southwestern United States, J. Appl. Meteorol. 17 (1978) 832–845.

[13] R.T. Matsumura, R.G. Flocchini, T.A. Cahill, O. Carvacho, Z. Lu, Measurement of fugitive PM10 emissions from selected agricultural practices in the San Joaquin Valley, in: J.C. Chow, D.M. Ono (Eds.), PM10 Standards and Nontraditional Particulate Source Controls, vol. I, Air and Waste Management Association, A&WMA/EPA International Specialty Conference, 1992, pp. 417–432.

[14] D.A. Gillette, T.R. Walker, Characteristics of airborne particles produced by wind erosion of sandy soil, High Plains of west Texas, Soil Sci. 123 (1977) 97–110.

[15] W.G. Nickling, Grain-size characteristics of sediment transported during dust storms, J. Sediment. Petrol. 53 (1983) 1011–1024.

[16] D.W. Fryrear, Soil losses by wind erosion, Soil Sci. Soc. Am. J. 59 (1995) 668–672.

[17] J.A. Gillies, W.G. Nickling, G.H. McTainsh, Dust concentrations and particle-size characteristic of an intense dust haze event: inland delta region, Mali, West Africa, Atmos. Environ. 30 (1996) 1081–1090.

[18] J.F. Leys, G.H. McTainsh, Sediment fluxes and particle grain-size characteristics of wind-eroded sediments in southeastern Australia, Earth Surf. Proc. Landforms 21 (1996) 661–671.

[19] J.E. Stout, T.M. Zobeck, The Wolfforth field experiment: a wind erosion study, Soil Sci. 161 (1996) 616–632.

[20] D.A. Gillette, D.W. Fryrear, T.E. Gill, T. Ley, T.A. Cahill, E.A. Gearhart, Relation of vertical flux of particles smaller than 10 μm to total aeolian horizontal mass flux at Owens Lake, J. Geophys. Res. 102 (D22) (1997) 26009–26016.

[21] K.E. Saxton, D. Chandler, L. Stetler, B. Lamb, C. Clairborn, B.H. Lee, Wind erosion and fugitive dust fluxes on agricultural lands in the Pacific Northwest, Trans. ASAE 43 (2000) 623–630.

[22] L. Gomes, J.L. Arrue, M.V. Lopez, G. Sterk, D. Richard, R. Garcia, M. Sabre, A. Gaudichet, J.P. Frangi, Wind erosion in a semiarid agricultural area of Spain: the WELSONS project, Catena 52 (2003) 235–256.

[23] D. Ono, S. Weaver, K. Richmond, Quantifying particulate matter emissions from wind blown dust using real-time sand flux measurements, in: Proceedings of the 12th International Emissions Inventory Conference, San Diego, CA, 2004, USEPA Tech Transfer Network website: http://www.epa.gov/ttn/chief/conference/ei12/index.html, 2004 (visited June 24, 2004).

[24] J.F. Kjelgaard, D.G. Chandler, K.E. Saxton, Evidence for direct suspension of loessial soils on the Columbia Plateau, Earth Surf. Proc. Landforms 29 (2004) 221–236.

[25] Y. Shao, M.R. Raupach, P.A. Findlater, Effect of saltation bombardment on the entrainment of dust by wind, J. Geophys. Res. 98 (1993) 12719–12726.

[26] D.A. Gillette, Fine particulate emissions due to wind erosion, Trans. ASAE 20 (1977) 890–897.

[27] Soil Survey Staff, Keys to Soil Taxonomy, 8th ed., USDA, Natural Resource Conservation Service, Washington, DC, 1998, p. 326.

[28] V.T. Holliday, Stratigraphy and Paleoevironments of Late Quaternary Valley Fills on the Southern High Plains, Geological Society of America, Memoir, vol. 186, 1995, p. 136.

[29] D.W. Fryrear, Soil ridges-clods and wind erosion, Trans. ASAE 27 (1984) 445–448.

[30] D.W. Fryrear, A field dust sampler, J. Soil Water Conserv. 41 (1986) 117–120.

[31] T.M. Zobeck, Field measurement of erosion by wind, in: R. Lal (Ed.), Encyclopedia of Soil Science, Marcel Dekker, Inc., New York, 2002, pp. 503–507.

[32] P. Stockton, D.A. Gillette, Field measurements of the sheltering effect of vegetation on erodible land surfaces, Land Degrad. Rehabil. 2 (1990) 77–85.

[33] J.C. Kaimal, J.J. Finnigan, Atmospheric Boundary Layer Flows, their Structure and Measurement, Oxford University Press, New York, 1994, pp. 14–19.

[34] J.E. Stout, A method for establishing the critical threshold for aeolian transport in the field, Earth Surf. Process. Landforms 29 (2004) 1195–1207.

[35] J.L. Rajot, S.C. Alfaro, L. Gomes, A. Gaudichet, Soil crusting on sandy soils and its influence on wind erosion, Catena 53 (2003) 1–16.

[36] SAS Institute, SAS/STAT User's Guide, Version 8.2, SAS Institute, Cary, NC, 1999, p. 3884.

[37] T.A. Cahill, T.E. Gill, J.S. Reid, E.A. Gearhart, D.A. Gillette, Saltating particles, playa crusts and dust aerosols at Owens (dry) Lake, California, Earth Surf. Process. Landforms 21 (1996) 621–639.

[38] S. Ravi, P. D'Ordorico, T.M. Over, T.M. Zobeck, On the effect of air humidity on soil susceptibility to wind erosion: the ease of air-dry soils, Geophys. Res. Lett. 31 (2004) L09501, doi:10.1029/2004g109485.

[39] J.A. Gillies, L. Berkofsky, Eolian suspension above the saltation layer, the concentration profile, J. Sediment. Res. 74 (2004) 176–183.

[40] W.S. Chepil, R.A. Milne, Comparative study of soil drifting in the field and in a wind tunnel, Sci. Agric. 19 (1939) 249–257.

[41] J.E. Stout, Wind erosion within a simple field, Trans. ASAE 33 (1990) 1597–1600.

[42] D.A. Gillette, G. Herbert, P.H. Stockton, P.R. Owen, Causes of the fetch effect in wind erosion, Earth Surf. Process. Landforms 21 (1996) 641–659.

[43] Z. Dong, H. Wang, X. Liu, X. Wang, The blown sand flux over a sandy surface: a wind tunnel investigation on the fetch effect, Geomorphology 57 (2004) 117–127.

[44] D.E. Buschiazzo, T.M. Zobeck, S.B. Aimar, Wind erosion in loess soils of the semiarid Argentinian Pampas, Soil Sci. 164 (1999) 133–138.